

A stepped frequency GPR system for underground prospecting

Giovanni Alberti, Luca Ciofaniello, Marco Della Noce, Salvatore Esposito, Giovanni Galiero,
Raffaele Persico, Marco Sacchettino and Sergio Vetrella

CO.RI.S.T.A., Consortium for Research on Advanced Remote Sensing Systems, Napoli, Italy

Abstract

In the framework of ARCHEO, a national research project funded by the Italian Ministry for Universities and Scientific and Technological Research (MURST), a new Ground Penetrating Radar (GPR) has been developed by the Italian Consortium for Research on Advanced Remote Sensing Systems (CO.RI.S.T.A.). The system has been specially designed to satisfy archaeological requirements and it will be used to identify and characterise buried objects. The system is a stepped frequency GPR. It can work within a wide band of frequencies both in gated and ungated mode, and it has been already widely described in Alberti *et al.* (2000). This paper describes the results of calibration tests in ungated mode performed in the CO.RI.S.T.A. laboratory. In particular, it is shown that the system can guarantee a dynamic range of about 96 dB.

Key words *stepped frequency – GPR*

1. Introduction

It is well known that electromagnetic waves propagate beyond the physical discontinuities that are between different media, and this makes it possible to investigate the internal features of dielectric (possibly lossy) bodies. An important aspect of this property is the possibility to investigate the presence of objects buried in the soil. With regard to this aspect, a number of experiments are reported, focused on hardware of GPR systems (Daniels, 1996; Stickley *et al.*, 1999; Alberti *et al.*, 2000) or possible kinds of

processing of GPR data (Kooij *et al.*, 1996; Bucci *et al.*, 2000; Pierri *et al.*, 2000; Wright *et al.*, 2000). There are, moreover, many papers focused mostly on the results of experimental campaigns performed (Colla *et al.*, 1995; Ferrucho da Rocha *et al.*, 2000; Meglich, 2000). In this paper, we focused on the aspect of the hardware of a GPR system developed by the Consortium for Research on Advanced Remote Sensing Systems (CO.RI.S.T.A.). This system was conceived within the framework of the scientific project ARCHEO, financed by Italian MURST and aimed to develop advanced devices and techniques to be used for detection and recovery of archaeological zones (Alberti *et al.*, 2000).

Before entering the subject of this paper, however, let us outline that, within the project ARCHEO, the data processing has been taken into account. The present system is equipped with a positioning system (Alberti *et al.*, 2000) that collects data in a multiview and multistatic configuration (and at several frequencies) in order to use an inverse scattering algorithm exploiting this measurement configuration (Persico *et al.*, 2000).

Mailing address: Ing. Giovanni Alberti, CO.RI.S.T.A., Consorzio di Ricerca su Sistemi di Telesensori Avanzati, Piazzale Tecchio 80, 80125 Napoli, Italy; e-mail: alberti@unina.it

Within ARCHEO, some instruments other than the GPR have also been designed (see the two papers by Fiorani *et al.*, 2000a,b), in order to have a more complete set of tools useful for archaeological purposes.

Before choosing to develop a stepped frequency GPR system, an investigation on some further non-destructive techniques available was conducted. The possibility to exploit seismic methods, inductive electromagnetic methods, magnetic methods, resistive methods and methods based on gravity strength were first studied (Alberti *et al.*, 2000) and the GPR technique was the most suitable for the purposes of ARCHEO. The final choice was a stepped frequency system because it ensures, with respect to the traditional impulsive GPR systems, a larger dynamic range and a greater signal to noise ratio, due to the larger amount of processed energy and to the narrow IF band (Noon, 1996). Moreover, a stepped frequency system is the most suitable instrument to gather data for a multifrequency inverse scattering algorithm (Persico *et al.*, 2000; Pierri *et al.*, 2000).

However, the choice of a stepped frequency system can be considered innovative because, although the advantages of the stepped frequency have been known since the seventies (Robinson *et al.*, 1974), most of the GPR systems currently adopted are still impulsive. To give a rough (but not meaningless) quantification of this statement, in the proceedings of the International GPR Congress of the years 1998 and 2000, there are two archaeological sections reporting only experiments performed with impulsive systems. Even the stepped frequency was deemed unsuitable for archaeological applications by Conyers and Goodman (1997), but without a precise justification.

Undoubtedly, the technology of impulsive systems is more assessed and therefore there are more manufacturers of impulsive systems (Daniels, 1996). However, we think that it is worth trying to exploit the theoretically better performances offered by the stepped frequency technology, that may only need some more efforts.

The GPR system at hand has been conceived to match some requirements specified by interacting with archaeologists (Festinese, 2000;

Signore, 2000). So, it was established that the radiation has to penetrate the soil to a depth of about three meters (in a dry soil), with a vertical resolution of 15 cm and a horizontal resolution of 50 cm. The system is conceived to look for dielectric targets like walls, floors, foundations, wells, ovens, temples, graves, roads and waterworks.

The system presented here can work both in ungated and gated mode, in order to exploit the greater dynamic range obtainable in ungated mode but also (in gated mode) to avoid saturation drawbacks due to the leakage or to strong reflections from very shallow objects (Noon, 1996; Stickley *et al.*, 1999). However, at the moment only laboratory tests in ungated mode are available.

The present paper is organised as follows: Section 2 describes the architecture of the system and Section 3 outlines some tests performed on the system in ungated mode, followed by conclusions and future developments.

2. Architecture of the system

In this section we show and explain the block diagram of the system. The scheme of the system is shown in fig. 1. To simplify the exposition, we deal with the ungated and the gated modes separately.

2.1. Ungated mode

In ungated mode, the two frequency synthesisers Tx and Rx (see fig. 1) generate two tones at distance 1 MHz on the frequency axis. The coherent oscillator (COHO) is not enabled and, consequently, the mixers R1 and S1 and the filters R1 and S1 are not enabled either (the signal bypasses them). A small part of the signal generated by the Tx transmitter is picked up by a directional coupler and is combined by the mixer S1 with half of the signal generated by the Rx synthesiser, picked up by a power splitter. Analogously, the signal received by the Rx antenna is combined, by the mixer R2, with the other half of the signal generated by the Rx synthesiser. The filters S2 and R2 have the task to reject the harmonic components at frequency

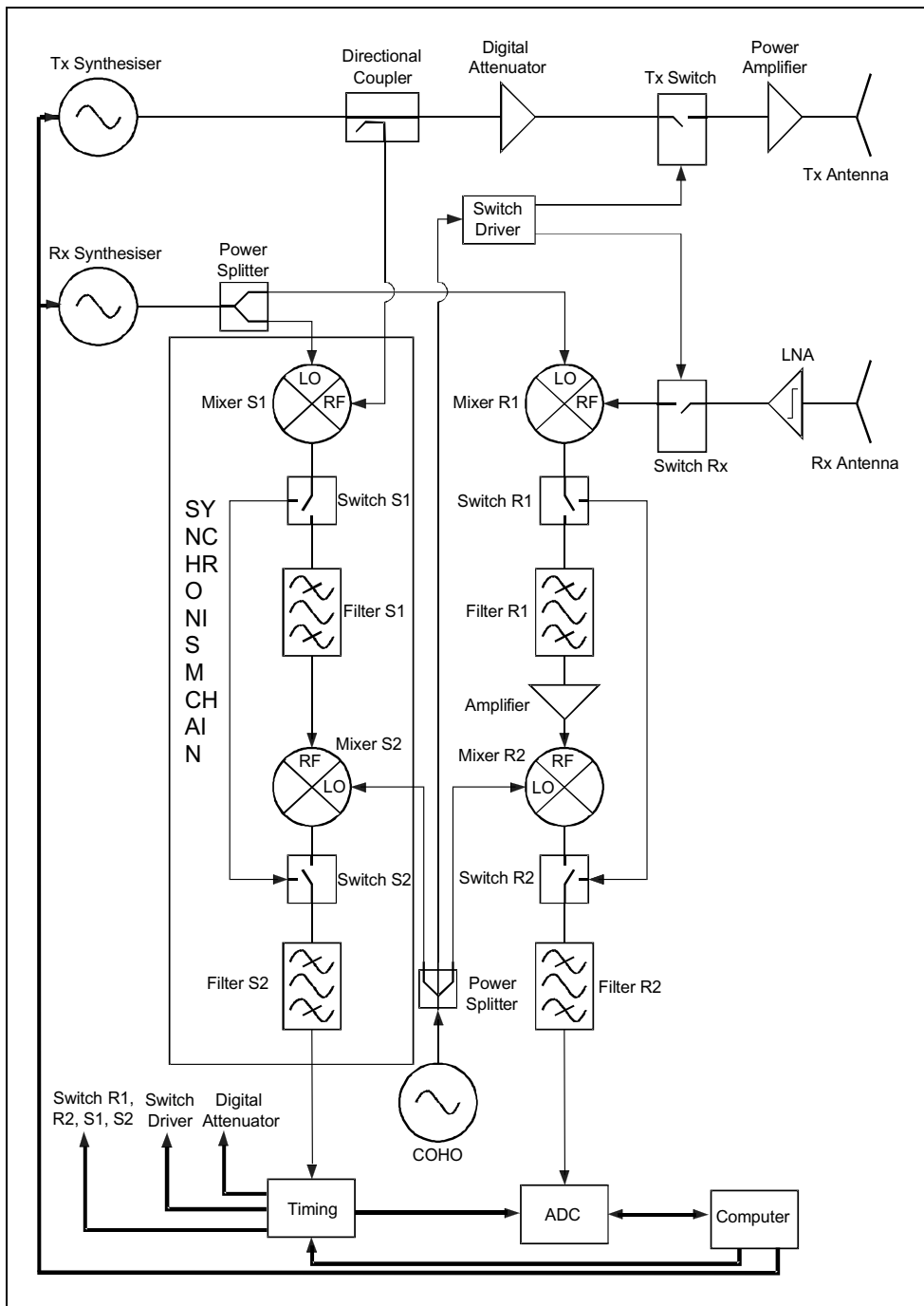


Fig. 1. Block diagram of the GPR system.

Table I. Some of the main characteristics of the system.

Frequency range of the radiated waves	100-900 MHz
Frequency range of the synthesizers	10 kHz-1 GHz
Frequency resolution of the synthesizers	0.2 Hz
Length of a single frequency step	From 10 μ s up to 10 s
Intermediate frequency for both gated and ungated modes	1 MHz
COHO frequency for the gated mode	100 MHz
Resolution of the ADC	23 bit
Band of the filter R1	2 MHz
Band of the filter R2	25 kHz
Band of the filter S1	12 MHz
Band of the filter S2	140 kHz
Range of the output power level of the synthesizers	From -137 dBm up to 13 dBm
Power level resolution of the synthesizers	0.1 dB
Maximum switching time of the synthesizers	15 s
Maximum number of steps of the synthesizers	8192
Nominal dynamic range of the ADC	More than 100 dB
Maximum sampling ratio of the ADC	20 MHz
Power at the antenna feed point	Up to 10 W
Size of the positioning system	320 \times 320 \times 100 cm ³
Resolution of the positioning system	1 cm

sum. So, the signals in output of the two filters (when a steady condition is reached) are two tones at 1 MHz, whose phase difference is related to the electrical path of the signal into the soil (once the electrical path inside the system is excluded by calibration). The bandwidths of the filters S2 and R2 are different (see table I). In particular, the bandwidth of S2 is the larger one, so to make the filter faster in reaching the steady condition at each of the swept frequencies. In fact, this output has to provide, by passing through the timing system, the clock signal to sample the 1 MHz tone at the output of the filter R2. The sampling clock is implemented by a frequency triplication followed by a threshold device, both included in the timing system. The wider bandwidth of the filter S2 with respect to the filter R2 also implicates the theoretical possibility that a stronger noise affects the output of S2. This is not a severe problem, because S2 is on the synchronism chain, and therefore the signal at its input only has propagated inside the

system. The signal at the input of the filter R2, instead, can be corrupted by external kinds of noise or interference or clutter gathered by the receiving antenna. This is the reason why the two filters have different bandwidths.

Apart from these specifications, the overall result provided by the system is a tone at 1 MHz (at the output of the filter R2) sampled with three samples out of a period, and this for each of the radiated frequencies. The discrete data so obtained can be averaged at each frequency and then stored. After this storage, an inverse FFT can provide the response to the radiated synthetic pulse (Daniels, 1996; Noon, 1996).

2.2. Gated mode

In the gated mode, the reception is inhibited while radiating the signal and the radiating is inhibited while receiving. This is done by a switch signal provided by the computer syn-

chronised with the COHO at 100 MHz, in the sense that the switch happens after a certain (integer) number of periods of the COHO, and this number is established via computer. In gated mode, the two synthesisers produce two tones at distance 101 MHz on the frequency axis. Therefore, after the first mixing and filtering there are two signals centred on the frequency 101 MHz, one on the receiving chain (at the output of the filter R1) and the other on the synchronism chain (at the output of the filter S1). In particular, R1 is an antialiasing filter aimed not only to attenuate the component at frequency sum (which is obvious) but also to reject the possible image band centred about the frequency 99 MHz. Therefore, the bandwidth of the filters R1 is 2 MHz (centred about 101 MHz). Again, the first filter on the synchronism chain is allowed to have a larger bandwidth (and therefore to be faster in reaching the steady condition), because the signal does not pass through an external path, and so one can reasonably suppose that there is no image band to be rejected. After the first mixing and filtering, the signal on the receiving chain and the signal on the synchronism chain are mixed again with the tone at 100 MHz provided by the COHO. So, after the second filtering (which is performed by the same filters exploited in the ungated mode) there are two tones at 1 MHz, likewise the ungated mode. The processing on these two tones is the same as that for the ungated mode.

3. Tests performed in ungated mode

As a first test, we measured the noise introduced by the clock that we have implemented within the timing system. In fact, this clock is a possible bottleneck for the dynamic range of the overall system (Sheer, 1993). Incidentally, other components were also tested, although specialised manufacturers guaranteed them. In particular, the ADC is by HP and is equipped with a high quality internal clock at 20 MHz. However, the internal clock of the ADC cannot be adopted within the overall system because it is needed to synchronise the sampling of the received signal with the transmitted signal, which requires a dedicated device. In particular, the

frequency switches are associated with some random phase shift of the transmitted signal, which needs the exploitation of a synchronism signal that «follows» the same shifts. This is why the acquisition is driven by the synchronism chain.

In order to measure the noise introduced by the timing system, the output of the filter R2 was disconnected from the ADC (see fig. 1). In these conditions there is no signal coming from the receiving chain and the signal delivered to the computer is the noise introduced by the clock. Instead, if the clock of the timing system is not enabled, whereas the internal clock of the ADC is enabled, the output delivered to the computer is the noise that would introduce the internal clock of the ADC if it could be adopted. As said, the clock internal to the ADC cannot be adopted, but the measure of its noise is interesting for comparison purpose. The noise introduced by the clock of the timing system is shown in fig. 2, and the noise introduced by the internal clock of the ADC is shown in fig. 3. In figs. 2 and 3 the average power of the noise is measured *versus* the frequency all over the band of the system. For the tests shown in figs. 2 and 3, a full scale of -6dBm was adopted for the input of the ADC. This is a trial value: in general the full scale adopted is a compromise between the need to retrieve signals as weak as possible and to reduce the probability of truncation of too strong signals. As can be seen, the noise introduced by the timing system is of the same order as the noise of the ADC internal clock (just a few dB stronger). In particular, this noise level guarantees a dynamic range of at least 93 dB (corresponding about to 16 bits).

This noise level can be further decreased if some averaging is performed on the data. Figure 4 shows the noise signal of the timing system, after an average performed on 32 samples (at each frequency) whereas fig. 5 shows the homologous quantity referred to internal clock of the ADC. We are speaking of an average performed via software. Actually, the ADC already performs via hardware some averaging which we do not dwell upon, but that is to be quoted for sake of completeness. In particular, it can reliably be assumed that each of the samples that reaches the computer (to be stored and/or

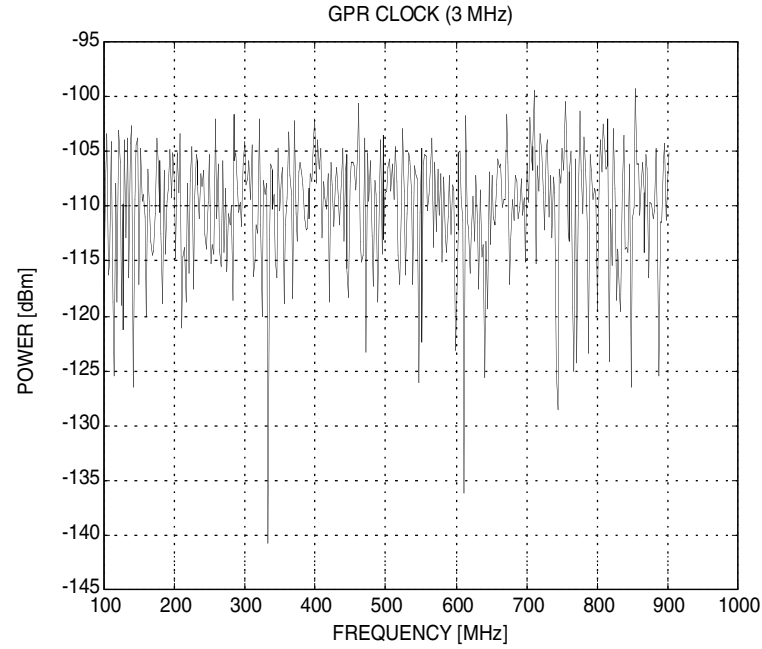


Fig. 2. Noise generated by the timing system.

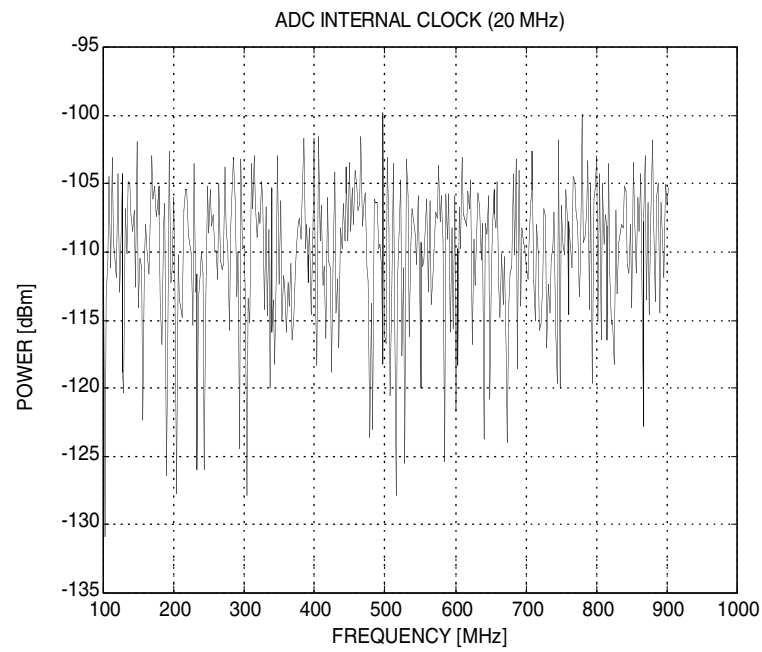


Fig. 3. Noise generated by the clock internal to the ADC.

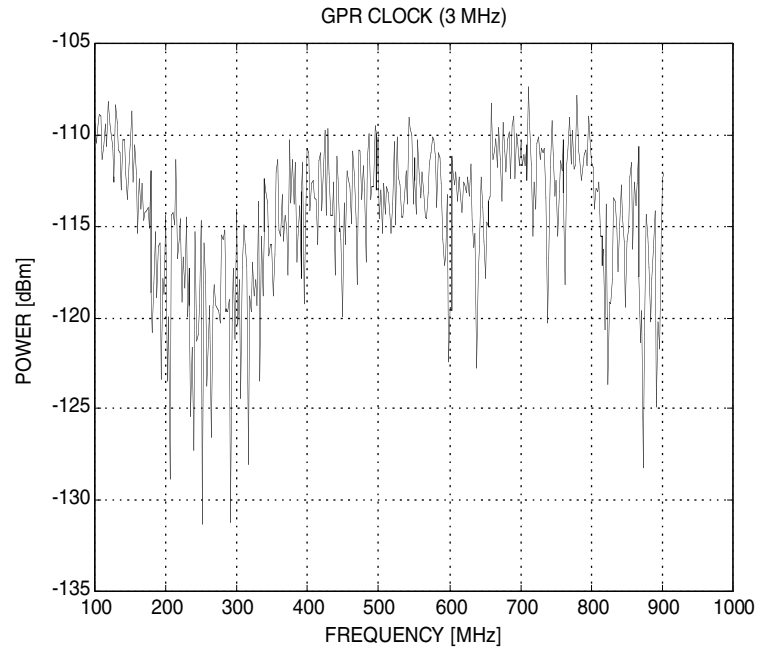


Fig. 4. Result of an averaging performed on the noise generated by the timing system.

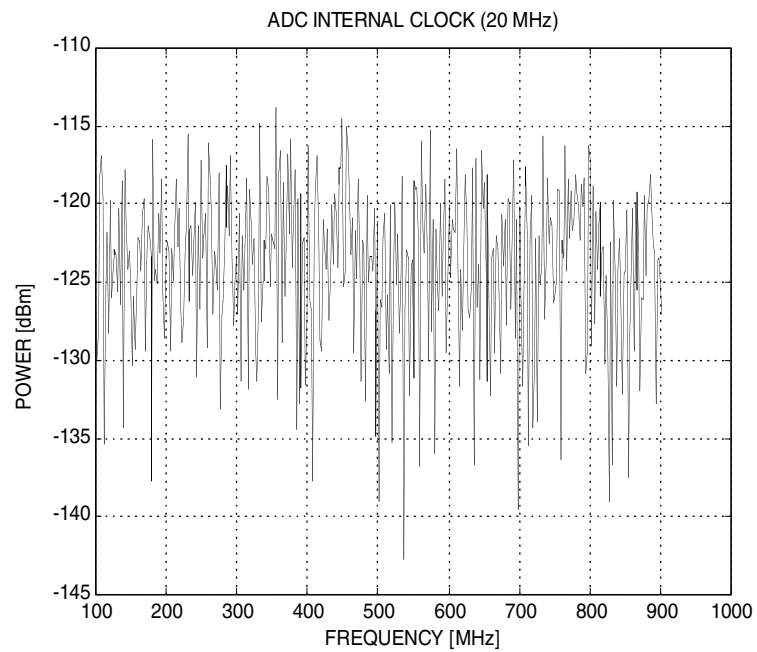


Fig. 5. Result of an averaging performed on the noise generated by the clock internal to the ADC.

processed) represents a sample of the steady condition harmonic response of the system at the current frequency. In other words, we can be confident that there is no meaningful transient effect in the samples in input at the computer.

It can be seen that the noise introduced by our clock guarantees a dynamic range of about 103 dB, and that of the internal clock of the ADC would guarantee a dynamic range only slightly larger (let say about 108 dB). On the other hand, this test also shows that a sort of spurious modulation appears superimposed on the noise signal generated by the clock of the GPR. This indicates that the behaviour of the averaged noise is going to reach some steady condition. Therefore, it is hopeless to think that an average on many more samples would provide further dramatic improvements: only a very few further dB might be obtained, at the cost of making the acquisition time twice longer if not even more.

Let us now show some tests performed on the coupling. The term «coupling» is meant to indicate all the spurious signals that enter the ADC from the receiving chain and that are due to the electromagnetic interaction by the different electronic components of the system. To quantify this coupling, for a fixed value of the power of the signal generated by the Tx synthesiser (precisely 5 watt, corresponding to 37 dBm), the receiving antenna was removed and the relative coaxial cable connected to a matched load. Moreover, the output of the filter R2 was again connected to the ADC (see fig. 1). In these conditions, the signal that enters the ADC from the receiving chain is substantially due to spurious electromagnetic couplings internal to the system itself.

Figure 6 shows the coupling signal recorded *versus* the frequency, with a full scale of -6 dBm (which is again a trial value). In fig. 6 no average on the output samples is performed: the shape itself of the signal makes us understand that there is a very little «degree of randomness», and therefore any averaging is substantially useless with regard to the coupling. As an explicit verification, fig. 7 shows the coupling signal after an averaging performed on 32 samples. The reason for this uselessness of the averaging is that the coupling signal reaches the

ADC by passing through the narrow-band filter R2. Therefore, the coupling is by its own nature a somewhat-averaged signal. There is an important difference between the noise introduced by the clock and the coupling: the former is meaningfully dependent on the quantization introduced by the ADC, because it substantially results in a sampled quantization noise. Instead, the coupling is related to the power level of the signal produced by the Tx synthesiser (that, let us remember, has been fixed at 5 watt). Consequently, the noise of the clock is expected to depend on the full scale adopted, whereas the coupling does not. In other words, with regard to the clock noise, what can be considered as «absolute» is the dynamic range with respect to the full scale adopted whereas, with regard to the coupling, what is to be regarded as «absolute» is the noise level in dBm.

Based on these considerations, a suitable choice for the full scale of the ADC might be one that «shifts» the clock noise on the same level of the coupling. In these conditions, there will be the maximum dynamic range. In fact, a lower full scale would decrease the dynamic range available, because the coupling would remain unchanged. On the other hand, a larger full scale would not enlarge the dynamic range because the clock noise would follow the increasing of the full scale. Actually, it might be useful to increase the full scale only if the truncation probability were greater than the probability to receive a signal weaker than the ADC resolution.

In the situation at hand, the full scale that makes equal to each other the power level of the clock noise and that of the coupling is 24 dBm, corresponding to 0.25 watt. Received signals stronger than this level are extremely improbable in our applications, because the power radiated is less than 5 watt whereas the attenuation encountered can be expected of the order of several tens of dB even if a reflection at less than one meter occurs (Noon, 1996). To be more precise, the overall attenuation and amplification between the Tx synthesiser and the transmitting antenna compensate each other, so the incident power at the input terminal is nominally 5 watt. Therefore, the radiated power can only be lower than this value, due to some unavoidable mismatch and losses in the antenna. With the choice of a full scale of 24 dBm, fig. 8 shows the comprehensive

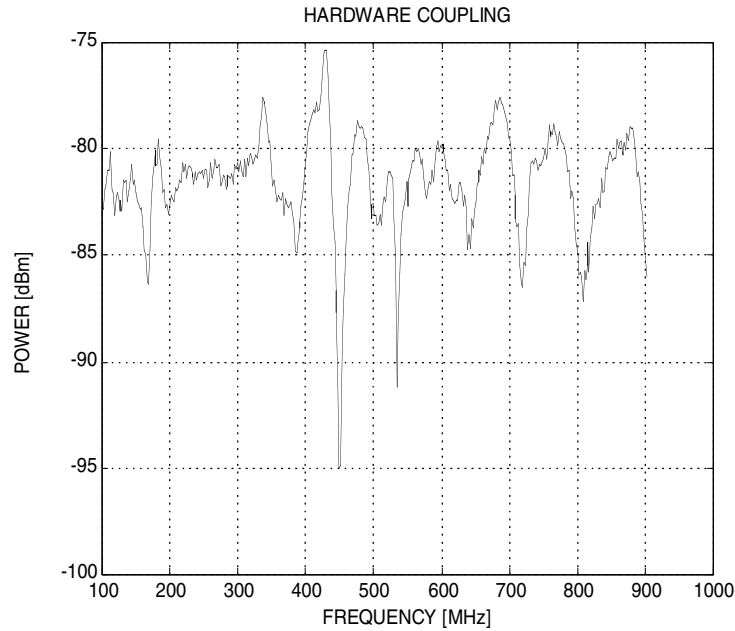


Fig. 6. Electromagnetic coupling internal to the GPR system.

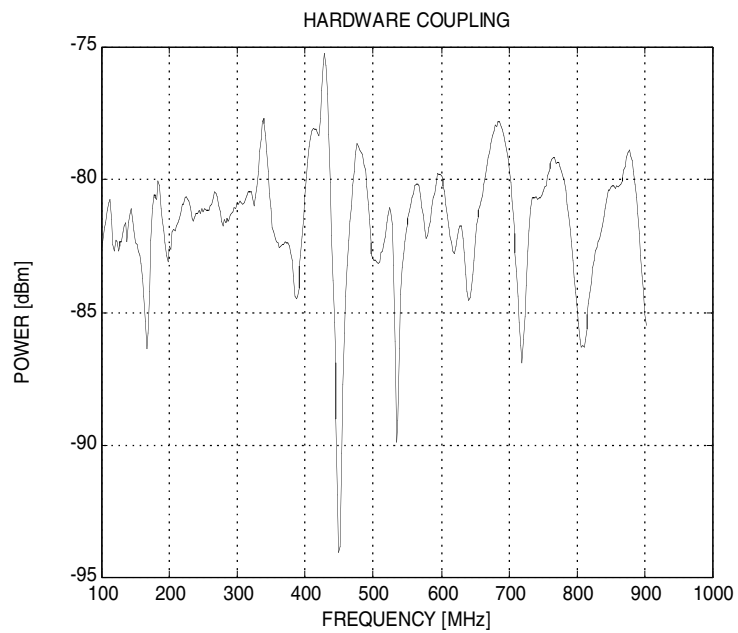


Fig. 7. Result of an averaging performed on the electromagnetic coupling.

noise (coupling plus clock) recorded at the output of the ADC. In fig. 8, no average is performed on the data: the weakest signal that can be recovered is at level of -66 dBm, and therefore the dynamic range can be quantified at 90 dB. However, if an average on 32 samples is performed, then the dynamic range grows to 94 dB, as can be understood by glancing at fig. 9. For most of the radiated frequencies, the dynamic range can be considered equal to 96 dB or even more, therefore it is not unfair to assess that that dynamic range is indeed about 96 dB.

Again, an average performed on many more samples is not expected to provide dramatic improvements of the dynamic range because, as said, the randomness of the clock noise has already been reduced and, above all, the averaging does not influence the coupling meaningfully.

Let us now show some tests on the phase and amplitude error at each frequency. These tests are relative both to the noise and to the possible distortion phenomena arising inside the system, that could deform the shape and position of the expected returned synthetic pulse.

In particular, in the performed tests the nominal harmonic signals generated have all been of the same amplitude, and therefore the theoretical received synthetic pulse is expected to be sinc-like. In order to test it, the two antennas were removed (see fig. 1) and the input of the transmitting antenna connected to the output of the receiving antenna with a coaxial cable that only introduces a known delay. In this manner the delay introduced by the overall GPR system was also measured, for calibration purposes. By this insertion, the theoretical signal to be received is known, based on the knowledge of the generated signal and on the knowledge of the components of the system. Therefore we can compare the received signal with the theoretical one. Figure 10 shows the relative amplitude error *versus* the frequency, whereas fig. 11 shows the phase error. Since the phase error is not a relative error but an absolute error, its effective entity cannot be evaluated by simply glancing at its behaviour. Rather, some criterion is to be introduced to evaluate the weight of this phase error. To do this, the

synthetic pulse received and the theoretical one can be compared: the discrepancy between them provides a quantification of the effects of the phase (and amplitude) error. Figure 12 reports these two pulses. In particular, the test pulse in fig. 12 is synthesised by switching the frequency of the Tx synthesiser from 100 MHz up to 902 MHz with a step of 2 MHz. Moreover, 64 samples were collected at each frequency, and the average of the last 20 samples were stored as the response of the system to the current frequency. To retrieve the synthetic pulse from the amplitude and the phase at each frequency, an IFFT on 8192 points was performed (Daniels, 1996; Noon, 1996). The ideal pulse is depicted as a solid line, whereas the actual recorded one is depicted in a dotted line: they are almost indistinguishable. To provide a worst case result, we show the ideal and the recorded synthetic pulse that we have (for the same experimental data) if only the frequencies from 802 up to 902 MHz are processed in retrieving the synthetic pulse. In fact, while the percentage amplitude error is quite low throughout the band (fig. 10), the higher frequencies of the swept band are those with a higher phase error. The result is shown in fig. 13 (again, the ideal pulse is in solid line whereas the actual pulse is in dotted line). The difference between them is slightly more evident on the secondary lobes, but substantially the main lobe remains unperturbed.

Finally, we show a test on the whole system working in ungated mode, *i.e.* a system with the overall system (including the antennas) mounted and working. We have looked for the reflection from the bottom of the floor of the laboratory in which the system (including the positioning system) is mounted. In fact, since there is another room under the laboratory, if the system is made to work in such a situation (with the two antennas positioned on the floor) the main reflection is expected from the ceiling of the room below. To synthesise the pulse, a band of 512 MHz was exploited, swept with a step of 2 MHz starting from the frequency of 100 MHz. The laboratory is a small (a surface of 5.7×3.6 m 2 and a tallness of 3.3 m) non anechoic environment, with the possibility of several multiple reflections from the walls, floor, ceiling, and the many metallic and dielectric objects present

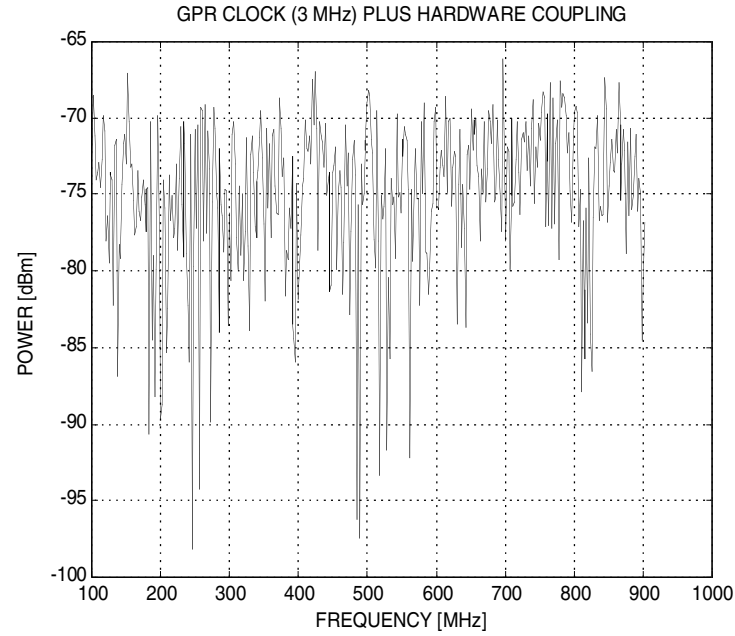


Fig. 8. Electromagnetic coupling plus timing system's noise.

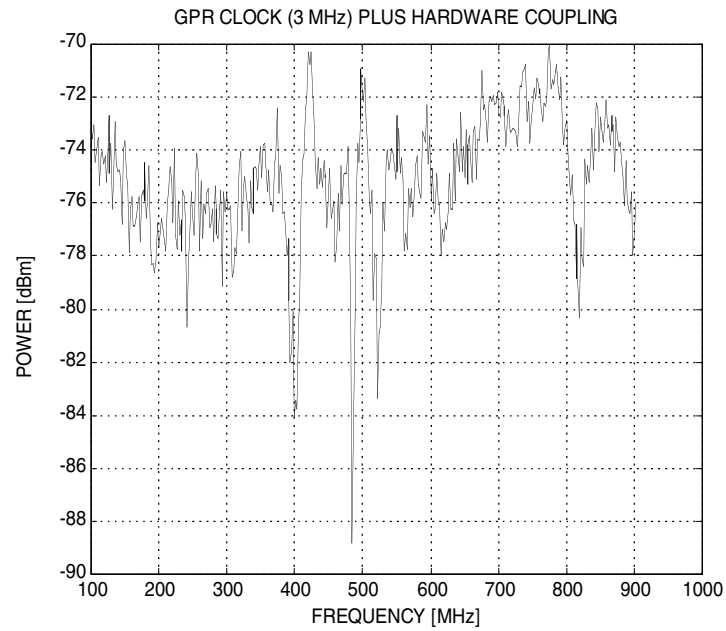


Fig. 9. Result of an averaging performed on the sum of the electromagnetic coupling and the noise generated by the timing system.

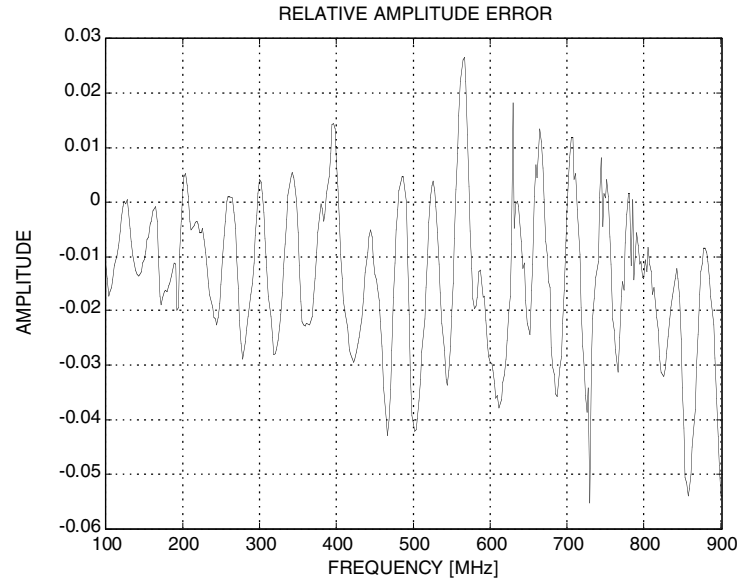


Fig. 10. Relative error (dB) between the nominal and the registered amplitude of a test signal *versus* frequency.

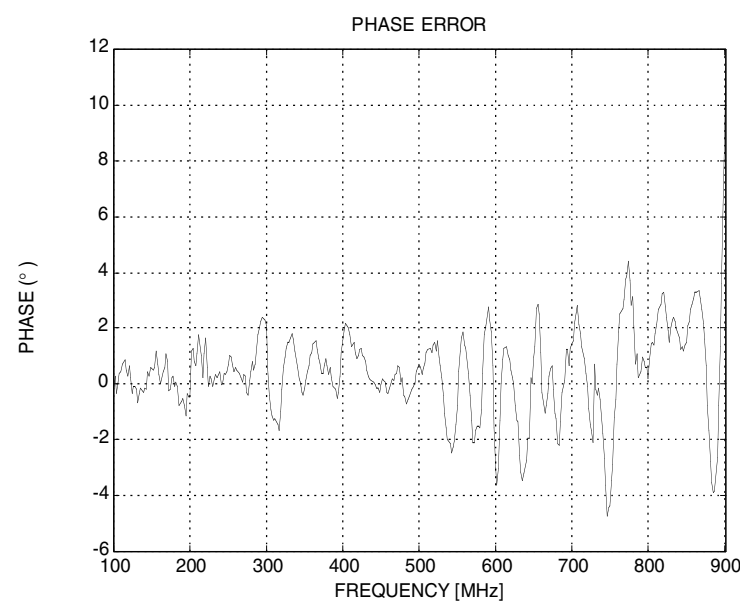


Fig. 11. Absolute error (degrees) between the nominal and the registered phase of a test signal *versus* frequency.

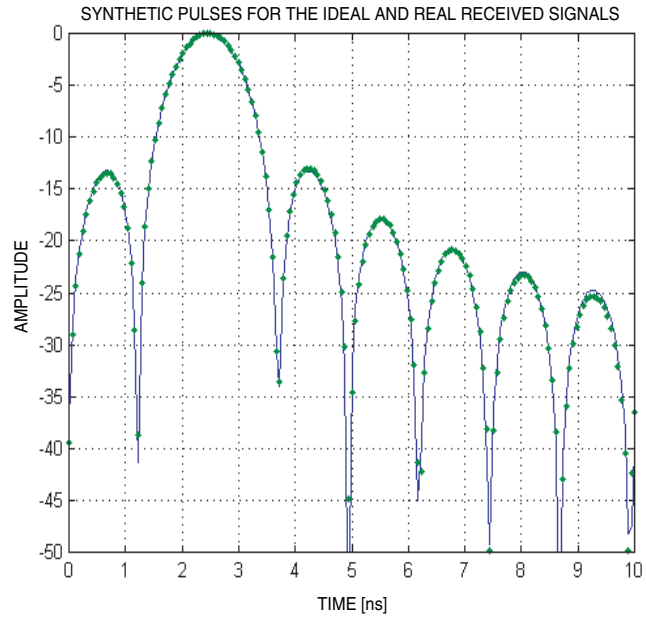


Fig. 12. Comparison of theoretical and received synthetic pulses making use of the stepped frequency signal on the overall band.

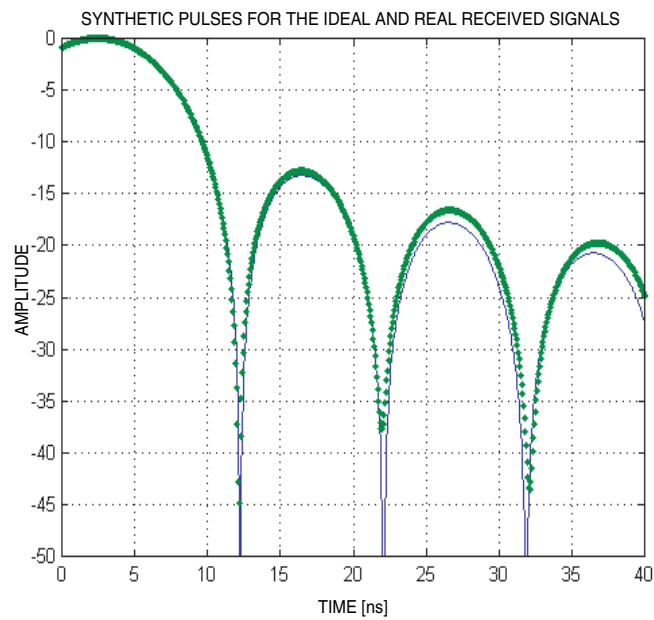


Fig. 13. Comparison of theoretical and received synthetic pulses making use of the stepped frequency signal on the «worst band» between 802 and 902 MHz.

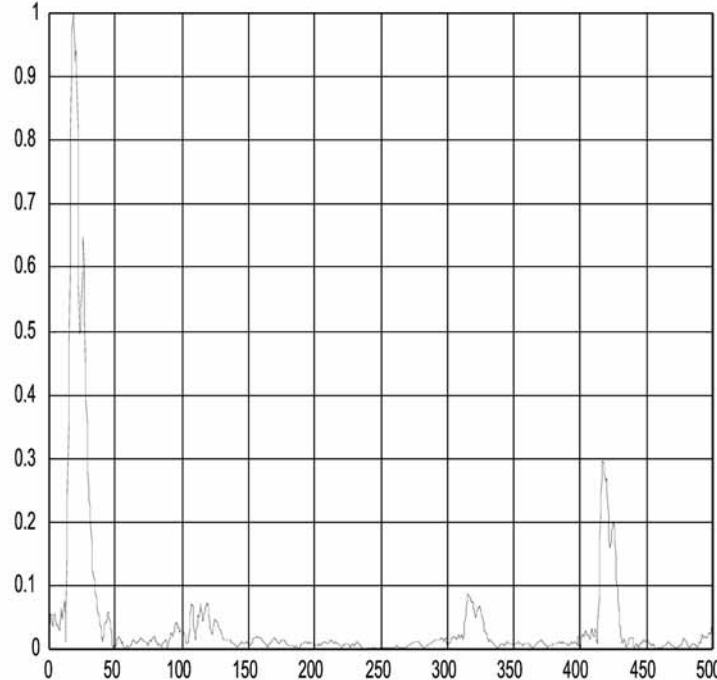


Fig. 14. One of the received synthetic time responses gathered in the laboratory of CO.RI.S.T.A. The function is normalised and expressed as a function of time in ns.

in the laboratory. Therefore, the conditions for this kind of measurement are not favourable at all. On the other hand, there is the *a priori* information that a reflection is expected from a plane surface parallel to the floor plane. The configuration of the measurement was in common source, and the receiving antenna was placed in eight different positions. The first four positions were arranged as follows: the receiving antenna was placed on one side of the transmitting antenna and the distance between the gaps was 40, 50, 60 and 70 cm respectively. The other four positions were chosen so that the receiving antenna was placed on the opposite site with respect to the transmitting antenna at the same distances. Due to the particular case at hand, the *a priori* supposition that the main reflection always occurs at the same depth was adopted. Therefore, even if the measurement configuration is a common source, the data were processed as

if they were in common depth point, according to the scheme illustrated in the Appendix. Figure 14 reports one of the 8 synthetic time responses (the others show all a quite similar behaviour). There is a strong reflection at the time of 18 ns, but there is also a meaningful reflection at about 420 ns, probably due to the floor of the underlying room. The depths worked out for all the distances (see Appendix) were averaged, and so the final result of 48 cm was worked out. The time values at which the various maxima occurred were exploited in working out the thickness of the floor.

Actually, the external wall of the building in which CO.RI.S.T.A. is located has zones where the plaster has fallen down, and therefore we were able to measure directly the thickness of the floor: it is 38.5 cm. Due to the bandwidth of the signal exploited, the uncertainty is expected of the order of 20 cm (see Appendix), and therefore the obtained result can be considered satisfactory.

4. Conclusions and future developments

A stepped frequency GPR system devised by the research consortium CO.RI.S.T.A. within the financed project ARCHEO has been described. The system can work both in ungated and gated mode and is equipped with a positioning system to allow measurements in a multistatic multiview configuration. Laboratory tests performed in the CO.RI.S.T.A. laboratory have been described. They show that the system is able to guarantee a dynamic range of the order of 96 dB in ungated mode. Following developments of the work, within the project ARCHEO, experimental tests will be performed in a pool filled with sand or

clay soil in which known buried targets will be buried (Alberti *et al.*, 2000). During the outdoor tests, innovative inverse scattering algorithms of the GPR data will also be tested (Persico *et al.*, 2000). Afterwards, the system is to be tested in an archaeological site in Southern Italy.

Acknowledgements

This study has been funded by the Italian Ministry for Universities and Scientific and Technological Research under research contract 179201-1325/458.

Appendix

This appendix outlines the processing performed to work out the thickness of the floor of the laboratory. As said, the processing was performed as if the data were gathered in a common depth point: therefore we refer to fig. 1A in order to explain the processing. The procedure is simple and conceptually similar to that exposed by Daniels (1996) for the case of a multimonostatic (common offset) configuration. With respect to fig. 1A, we have

$$p_1 = \sqrt{d^2 + l_1^2} \quad (\text{A.1})$$

$$p_2 = \sqrt{d^2 + l_2^2} \quad (\text{A.2})$$

for the Pythagorus theorem. Moreover

$$t_1 = \frac{2p_1}{c} \quad (\text{A.3})$$

$$t_2 = \frac{2p_2}{c} \quad (\text{A.4})$$

where c is the (unknown) propagation velocity of the electromagnetic radiation in the medium under consideration, assumed homogeneous.

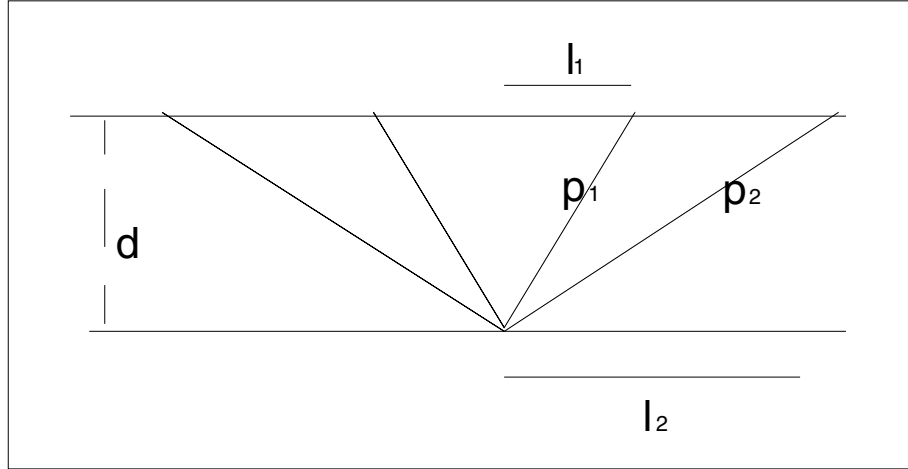


Fig. 1A. Geometrical scheme to retrieve the depth of a reflection from several measurements in common depth point.

Therefore, by substitution of (A.1) in (A.3) and (A.2) in (A.4), we obtain

$$\frac{t_1}{t_2} = \sqrt{\frac{d^2 + l_1^2}{d^2 + l_2^2}} \quad (\text{A.5})$$

The inversion of (A.5) with respect to d provides

$$d = \sqrt{\frac{l_1^2 t_2^2 - l_2^2 t_1^2}{t_1^2 - t_2^2}} \quad (\text{A.6})$$

Once d is retrieved, these passages allow retrieving the propagation speed c , by substitution of the known value of p_1 in (A.3) or p_2 in (A.4). In the case at hand, by averaging the 8 velocities obtained along the 8 electrical path considered, we have worked out $c = 10$ cm/ns. Once the propagation speed has been retrieved, one can estimate the order of magnitude of the spatial uncertainty as the product of this velocity times the temporal resolution. The temporal resolution can be estimated as $1/B$, where B is the bandwidth of the synthetic pulse (Daniels, 1996; Noon, 1996). In the case at hand, as said, the band is 512 MHz and so the temporal resolution is about 2 ns. Therefore the order of magnitude of uncertainty on the evaluation of the depth is 2 ns times 10 cm/ns, *i.e.* 20 cm. To be more precise, this calculation provides the uncertainty $2\Delta p$ on the length $2p$ of some average path of the signal within the floor (see eqs. (A.1) and (A.2) and fig. 1A), which is not d . By differentiating eq. (A.1) or (A.2) one might say that the uncertainty on the depth would be $\Delta d = (p/2d)\Delta p$, expected lower than $2\Delta p$ but of the same order of magnitude. On the other hand, this calculation neglects the uncertainty on the propagation velocity itself and the fact that, actually, the floor is not really homogeneous.

REFERENCES

- ALBERTI, G., L. CIOFANIETTO, M. DELLA NOCE, S. ESPOSITO, G. GALIERO, R. PERSICO and S. VETRELLA (2000): Advanced stepped frequency GPR development, in *Proceedings of the Conference on Subsurface Sensing Technologies and Applications II, at SPIE's Annual Meeting in July/August 2000, San Diego, U.S.A.*, 484-492.
- BUCCI, O.M., L. CROCCO, T. ISERNIA and V. PASCAZIO (2000): Inverse scattering problems with multifrequency data: reconstruction capabilities and solution strategies, *IEEE Trans. Geosci. Remote Sensing*, **38** (4), 1749-1756.
- COLLA, C., P. DAS, D. MCCANN and M. FORDE (1995): Investigation of stone masonry bridges using sonics, electromagnetics and impulse radar, in *Proceedings of International Symposium on Non-Destructive Testing Civil Engineering (NDT-CE), September 1995*, 629-636.
- CONYERS, L.B. and D. GOODMAN (1997): *Ground Penetrating Radar—an Introduction for Archaeologists* (Alta Mira Press, A division of Sage Publications).
- DANIELS, D.J. (1996): *Surface-Penetrating Radar*, The Institution of Electrical Engineers, London.
- FERRUCHO DA ROCHA, P.L., G. DA SILVA CEZAR and A. BUARQUE (2000): Archaeological sites at Rio de Janeiro State, Brazil, with their contents enhanced by the use of ground penetrating radar, in *Proceedings of the 8th International Conference On Ground-Penetrating Radar, Queensland, Australia*, 607-617.
- FESTINESE, C. (2000): Archeo-apparecchiature e tecniche avanzate per il rilevamento ed il recupero delle zone archeologiche, in «*Rischio Archeologico: se lo Conosci lo Eviti*, edited by M.P. GUERMANDI. *Proceedings of Convegno su Cartografia Archeologica e Tutela del Territorio, Ferrara, March 24-25 2000*», IBC, Documenti 31, Firenze 2001, 381-383.
- FIORANI, L., M. BORTONE, S. MATTEI, C. RUOCCHIO, A. SALOMÉ and S. VETRELLA (2000a): Miniaturized electro-optical sensors for archaeological prospecting, in *Proceedings of the Conference on Subsurface Sensing Technologies and Applications II, at SPIE's Annual Meeting in July/August 2000, San Diego, U.S.A.*, 442-446.
- FIORANI, L., M. BORTONE, S. MATTEI, C. RUOCCHIO, A. SALOMÉ and S. VETRELLA (2000b): Miniaturized laser range-finder for the volumetric characterization of underground cavities, in *Proceedings of the Conference on Subsurface Sensing Technologies and Applications II, at SPIE's Annual Meeting in July/August 2000, San Diego, U.S.A.*, 457-463.
- KOOU, B.J., M. LAMBERT and D. LESSELIER (1999): Non-linear inversion of a buried object in transverse electric scattering, *Radio Sci.*, **34** (6), 1361-1371.
- MEGLICH, T.M. (2000): Use of ground penetrating radar in detecting fossilized dinosaur bones, in *Proceedings of the 8th International Conference on Ground-Penetrating Radar, Queensland, Australia*, 536-541.
- NOON, D.A. (1996): Stepped-frequency radar design and signal processing enhances ground penetrating radar performance, *Ph.D. Thesis*, Department of Electrical and Computer Engineering, University of Queensland, Australia.
- PERSICO, R., G. ALBERTI, S. ESPOSITO, G. LEONE and F. SOLDOVIERI (2000): On multifrequency strategies of use of G.P.R. systems, in *Proceedings of the Conference on Image Reconstruction from Incomplete Data, at SPIE's Annual Meeting in July/August 2000, San Diego, U.S.A.*, 26-34.
- PIERRI, R., A. BRANCACCIO and F. DE BLASIO (2000): Multifrequency dielectric profile inversion for a cylindrically stratified medium, *IEEE Trans. Geosci. Remote Sensing*, **38** (4), 1716-1724.
- ROBINSON, L., W.B. WEIRAND and L. YUNG (1974): Location and recognition of discontinuities in dielectric media using synthetic RF pulses, *Proc. IEEE*, **62** (1), 36-44.
- SHEER, J.A. (1993): AA. VV.: *Coherent Radar Performance Estimation* (J.L. Kurts Editor, Artech House).
- SIGNORE, G.M. (2000): Progetto archeo: Cales, un'applicazione, in «*Rischio Archeologico: se lo Conosci lo Eviti*, edited by M.P. GUERMANDI. *Proceedings of Convegno su Cartografia Archeologica e Tutela del Territorio, Ferrara, March 24-25 2000*», IBC, Documenti 31, Firenze 2001, 384-390.
- STICKLEY, G.F., D.A. NOON, M. CHERNIAKOV and I.D. LONGSTAFF (1999): Gated stepped-frequency ground penetrating radar, *J. Appl. Geophys.*, **43** (2000), 259-269.
- WRIGHT, D.L., D.V. SMITH, J.D. ABRAHAM, R.S. HUTTON, E.K. BOND, T.J. CUI, A.A. AYDINER and W.C. CHEW (2000): Imaging and modelling new vetem data, in *Proceedings of the 8th International Conference on Ground-Penetrating Radar, Queensland, Australia*, 146-150.